NSG-695

X-611-66-365

THE PROPAGATION OF LOW ENERGY CHARGED PARTICLES IN THE INNER SOLAR SYSTEM

AUGUST 1966

GPO PRICE $ ______________

CFSTI PRICE(S) $ ______________

Hard copy (HC) 2.00

Microfiche (MF) .50

ff 653 July 65

NASA — GODDARD SPACE FLIGHT CENTER —

GREENBELT, MARYLAND

The Propagation of Low Energy
Charged Particles in the Inner Solar System

V. K. Balasubrahmanyan*
Goddard Space Flight Center
Greenbelt, Maryland

and

G. Skadron
University of Maryland
Department of Physics and Astronomy
College Park, Maryland

*On leave from Tata Institute of Fundamental Research, India.

Abstract

The effects of particle drift as well as diffusion and convection are employed to describe the propagation of solar charged particles in the inner solar system. It is found that protons and electrons gradient drift in opposite polar directions in the interplanetary magnetic field, and although the charge separation thereby produced is very small, this drift determines the energy loss of these particles. In addition, it is shown that electric field drift causes protons and electrons, alike, to corotate but slower than the magnetic field structure. As a result, solar particles injected onto a given magnetic field line sweep past the earth later than the field line. The resulting azimuthal intensity profile is determined by the distribution of sun-earth transit times for these particles as they diffuse along the magnetic field lines. These considerations are applied to low energy protons and electrons and predictions for their energy loss and intensity profiles are made. A comparison of these predictions with the data from the Imp I satellite indicates that the observed recurrent protons might be understood in terms of this analysis if the diffusion is sufficiently slow to give 1 Mev protons a 4 day transit time. The observed electrons, however, cannot have had such a solar origin and are evidently galactic.

I. Introduction

In order to correctly understand the properties of galactic cosmic rays and particles of solar origin it is necessary to understand the effects produced on these particles by passing through the interplanetary field and solar plasma. This problem has, of course, been extensively studied for years and has been reviewed in detail by Parker (1963).

During recent years much has been learned about the solar wind and the interplanetary field, and this has now made possible detailed studies of the propagation of charged particles through the solar system. In particular during 1963-1964, the Imp I satellite provided extremely valuable data by carrying detectors which simultaneously made measurements on the interplanetary magnetic field (Wilcox and Ness, 1965), the solar plasma (Bridge, et al, 1965), low energy protons (Fan, et al, 1966) and electrons (Cline, et al, 1964) and galactic cosmic rays (Balasubrahmanyan, et al, 1965). The data from Imp I which is of interest to us in the present work is shown in Figure 1. At that time the interplanetary magnetic field formed four sectors of alternating polarity whose boundaries are indicated in the figure by vertical lines. (These lines appear cross hatched when the exact time of passage of the sector boundary is uncertain due to the satellites being near perigee.) As one can see, low energy protons, which evidently do not originate from observable solar flares (Fan, et al, 1966), were observed to recur in a particular positive magnetic sector while electrons of comparable energy seemed to recur predominantly in an adjacent negative magnetic sector. Also shown in the figure is the counting rate for galactic cosmic rays above 50 Mev/nucleon and the bulk velocity of the solar wind.

The observed association of recurrent particle beams with magnetic sectors of fixed polarity lead us to examine the possibility that these Mev particles are released from the sun preferentially along a magnetic sector boundary and subsequently undergo a drift from that boundary. Sections II and III are therefore devoted to the description of particle drift in the interplanetary magnetic field and its relationship to the transport of particles between the sun and earth. Drift has ordinarily been discounted as being small for solar flare particles (Parker, 1963) (Axford, 1965); however we find that drift is of great significance in determining the energy loss as well as perhaps, the intensity-time profiles for events of the kind described above.

In the last section we investigate the possibility that the observed electron and cosmic ray time variations are simply the result of modulation by a variable solar wind. This has been done by evaluating the linear correlation coefficient between the daily particle intensity records and the plasma velocity records, and we find that cosmic rays, in particular, tend to follow the daily solar wind variations.

II. Drift in the Interplanetary Magnetic Field

We shall refer to a spherical coordinate system (r,θ,Φ) centered at the sun and at rest with respect to the earth and begin by considering the motion in the polar direction of charged particles ejected from a particular location (r_o,θ_o,Φ_o) on the solar surface. Assuming that the interplanetary magnetic field is reasonably regular in the inner solar system, the motion of protons and electrons of $\sim$10 Mev may be treated in the guiding center approximation. The most general drift velocity, to first order in the ratio of the Larmor radius to the field scale size, is given by Northrop (1963) as

$$\dot{R}_\perp = \frac{\bar{B}}{B^2} \times \left\{ - c\bar{E} + \frac{Mc}{e} \nabla |B| + \frac{mc}{e} \left(\dot{R}_\parallel \frac{d\hat{\epsilon}_1}{dt} + \frac{d\vec{u}}{dt} E \right) \right\} \tag{1}$$

where M is the particle's orbital magnetic moment, $\hat{\epsilon}_1$ is the unit vector along the magnetic field and $\mu_E = \frac{cE x B}{B^2}$. Approximating that the fields are static, the drift velocity becomes

$$\dot{R}_\perp = \frac{\bar{B}x}{B^2} \left\{ - c\bar{E} + \frac{Mc}{e} \nabla |B| + \frac{mc\dot{R}_\parallel}{e} \dot{R} \cdot \nabla \left(\frac{\vec{B}}{B}\right) \right\} \tag{2}$$

where the $\dot{R} \cdot \nabla \mu_E$ term, which is small, has been neglected.

The interplanetary magnetic field is assumed to have the underlying Archimedes spiral pattern (Parker 1963)

$$B_r = B_o \left(\frac{r_o}{r}\right)^2 , \quad B_\theta = 0 , \quad B_\phi = - \frac{\Omega r \sin\theta}{V_o} B_o \left(\frac{r_o}{r}\right)^2 \tag{3}$$

where B_o is the field at the sun, r_o is the solar radius, Ω is the solar angular velocity and V_o is the solar wind speed. Remembering that the solar wind is radial and that $E = -\frac{1}{c} V_o \times B$, equation 2 becomes

$$\dot{R}_{\perp} = \frac{\vec{B}}{B^2} \times \left\{ \left[\frac{Mc}{e}\frac{dB}{dr} + \frac{mc\dot{R}_{\parallel}}{e}\left(\dot{R}_r \frac{d}{dr}\left(\frac{Br}{B}\right) - \dot{R}_{\phi}\frac{B\phi}{rB}\right)\right]\hat{r} - B_{\phi} V_o \hat{\theta} \right.$$

$$\left. + \frac{mc\dot{R}_{\parallel}}{e}\left(\dot{R}_r \frac{d}{dr}\left(\frac{B\phi}{B}\right) + \dot{R}_{\phi}\frac{Br}{rB}\right)\hat{\phi} \right\} \qquad (4)$$

In obtaining equation 4, it has been approximated that B is independent of ϕ over the region of interest and that the phenomena at hand occur near the ecliptic plane ($\theta \sim \frac{\pi}{2}$). The polar drift velocity becomes

$$\dot{R}_{\theta} = \frac{Mc}{e}\frac{B\phi}{B^2}\frac{dB}{dr} + \frac{mc\dot{R}_{\parallel}\dot{R}_r}{eB^2}\left(B_{\phi}\frac{d}{dr}\left(\frac{Br}{B}\right) - Br\frac{d}{dr}\left(\frac{B\phi}{B}\right)\right) - \frac{mc\dot{R}_{\parallel}\dot{R}_{\phi}}{erB} \qquad (5)$$

Now the magnetic moment is given by $\frac{mv_{\perp}^2}{2|B|}$ and the guiding center velocity (which is approximately $v_{\parallel}$) has the components $\dot{R}_r = \frac{B_o}{|B_o|} V_{\parallel} \left(1 + \frac{\Omega^2 r^2}{V_o^2}\right)^{-1/2}$ and $\dot{R}_{\phi} = -\frac{\Omega r}{V_o}\frac{B_o}{|B_o|} V_{\parallel}\left(1 + \frac{\Omega^2 r^2}{V_o^2}\right)^{-1/2}$. Then by use of equation 3, one obtains

$$\dot{R}_{\theta} = \frac{m(V_{\perp}^2 + 2\,V_{\parallel}^2)\,c\Omega r^2 + \frac{1}{2}m(V_{\perp}^2 + 2\,V_{\parallel}^2)\,c\Omega r^2 \cdot \frac{\Omega^2 r^2}{V_o^2}}{eV_o\,B_o\,r_o^2\left(1 + \frac{\Omega^2 r^2}{V_o^2}\right)^2} \qquad (6)$$

We are interested in this drift velocity for $r \leq 1$ AU, corresponding to $\Omega r \leq V_o$, and in this case the second term may be neglected. Also we expect that magnetic irregularities in the field maintain a random pitch angle distribution for the particles, implying that on the average, $V_\perp^2 = 2V_\parallel^2$. We therefore approximate

$$\dot{R}_\theta \simeq \frac{mV^2\, c\,\Omega\, r^2}{e\, V_o\, B_e\, R_e^2 \left(1 + \frac{\Omega^2 R_e^2}{V_o^2}\right)^{-1/2} \left(1 + \frac{\Omega^2 r^2}{V_o^2}\right)^2} \tag{7}$$

where B_e is the magnitude and polarity of the magnetic field at 1 AU. This implies that protons and electrons of the same kinetic energy drift in the polar direction with equal speeds but in the opposite direction. If the magnetic field is outward ($B_e > 0$) equation 7 implies that protons drift south and electrons drift north, whereas the drift directions are reversed if the magnetic field is inward toward the sun. Therefore if protons and electrons are ejected from, say, the northern solar hemisphere, protons drift toward the ecliptic (and hence the earth) if the magnetic field is outward and electrons drift toward the ecliptic if the magnetic field is inward. It must be noted at this point that any drift in the polar direction by these particles implies a change of energy by an amount

$$d\mathcal{E} = eE_\theta\, r\, d\theta = eV_o\, B_\phi\, r\, d\theta = -\,10^{-8}\, e\,\Omega\, B_e R_e^2 \left(1 + \frac{\Omega^2 R_e^2}{V_o^2}\right)^{-1/2} d\theta \tag{8}$$

where B_e is in gauss, R_e in cm, and Ω in sec $^{-1}$. Defining $\mathcal{E}_o$ as the particle energy when at θ_o, $\mathcal{E}(\theta') = \mathcal{E}_o - c\,\theta'$; where $\theta' = \theta - \theta_o$ and $c = 10^{-8} e\,\Omega\, B_e R_e^2 \left(1 + \frac{\Omega^2 R_e^2}{V_o^2}\right)^{1/2}$. From equation 7 the angular drift velocity then becomes

$$\frac{d\theta'}{dt} = \frac{\dot{R}_\theta}{r} = \frac{2\, c\,\Omega\, r(\mathcal{E}_o - c\,\theta') \left(1 + \frac{\Omega^2 r^2}{V_o^2}\right)^{-2}}{eV_o\, B_e R_e^2 \left(1 + \frac{\Omega^2 R_e^2}{V_o^2}\right)^{-1/2}}$$

and

$$\frac{d\theta'}{dr} = \frac{d\theta'}{dt} \cdot \frac{1}{\frac{dr}{dt}} = \frac{1}{V_D(r,\theta')} - \frac{2\,c\Omega r(\mathcal{E}_o - c\theta')\left(1 + \frac{\Omega^2 r^2}{V_o^2}\right)^{-2}}{eV_o\, B_e R_e^2\left(1 + \frac{\Omega^2 R_e^2}{V_o^2}\right)^{-1/2}} \tag{9}$$

where $V_D(r,\theta')$ is the mean speed with which the particles move outward at r and θ'. Furthermore it follows from equations 6 and 8 that

$$\frac{d\mathcal{E}}{dt} = -c\frac{d\theta}{dt} = -c\frac{\dot{R}_\theta}{r} = -\frac{c}{r}\left[\frac{2(\mathcal{E}_\perp + 2\mathcal{E}_\parallel)\,\Omega r^2 + (\mathcal{E}_\perp + 2\mathcal{E}_\parallel)\Omega r^2 \cdot \frac{\Omega^2 r^2}{V_o^2}}{eV_o\, B_o\, r_o^2\left(1 + \frac{\Omega^2 r^2}{V_o^2}\right)^2}\right] \tag{9a}$$

This energy loss function has the limits,

$$\frac{d\mathcal{E}}{dt} = -\frac{2(\mathcal{E}_\perp + 2\mathcal{E}_\parallel)\Omega^2 r}{V_o} \qquad \text{for } \Omega r \ll V_o, \text{ and}$$

$$\frac{d\mathcal{E}}{dt} = -\frac{(\mathcal{E}_\perp + 2\mathcal{E}_\parallel)\,V_o}{r} \qquad \text{for } \Omega r \gg V_o\,.$$

and tells us that particles near the sun lose energy more slowly than has previously been thought (Parker, 1965).

We now consider the drift of particles in the azimuthal direction. From equation 4,

$$\dot{R}_\phi = -\frac{B_r\, B_\phi\, V_o}{B^2} = \frac{\Omega r}{1 + \frac{\Omega^2 r^2}{V_o^2}} \tag{10}$$

implying that electric drift causes the particles to corotate with the field structure near the sun, but slower than the field structure with increasing r. Relative to the field structure, the azimuthal drift velocity becomes

$$\dot{R}_{\phi'} = - \Omega r + \frac{\Omega r}{1 + \frac{\Omega^2 r^2}{V_o^2}} = - \frac{\Omega^3 r^3}{V_o^2 \left(1 + \frac{\Omega^2 r^2}{V_o^2}\right)} \tag{11}$$

and therefore

$$\frac{d\phi'}{dr} = \frac{1}{\frac{dr}{dt}} \frac{d\phi'}{dt} = \frac{1}{V_D} \frac{\dot{R}_{\phi'}}{r} = - \frac{\Omega^3 r^3}{V_D V_o^2 \left(1 + \frac{\Omega^2 r^2}{V_o^2}\right)} \tag{12}$$

where ϕ' is an azimuthal angle relative to the field structure and V_D is again the radial diffusion velocity. This function is considered in the following section.

III. Bulk Motion in the Interplanetary Field

A unified description of the simultaneous drift, convection and diffusion of particles propagating through the interplanetary medium can be obtained by constructing a Fokker-Planck transport equation for the problem. Letting $N(\bar{r}, \mathcal{E}, t)$ represent the number of particles/volume with energy $\mathcal{E}$ at the time t, and letting $\bar{j}$ represent the particle current density, the Fokker-Planck equation is

$$\frac{\partial N}{\partial t} + \nabla \cdot j + \frac{\partial}{\partial \mathcal{E}} (N \dot{\mathcal{E}}) = 0 ,$$

Diffusion, convection and drift all contribute to $\vec{j}$ so that

$$\vec{j} = \vec{j}_{diffusion} + \vec{j}_{convection} + \vec{j}_{drift}$$

Since the scale of the interplanetary field structure seems to be large compared with the Larmor radii we consider here, the particle motion is well approximated as a guiding along the force lines. But small scale irregularities in the magnetic field can be expected to produce non-adiabatic changes in the pitch angle (Roelof, 1966) and thus a particle tends to find itself with a mirroring pitch angle after some characteristic distance λ (the mean free path). This gives rise to a random walk along the lines of force and leads to the usual diffusion current,

$$j_{diffusion} = - K \nabla_b N \tag{13a}$$

The radial expansion of the solar wind convects the magnetic irregularities radially outward, but since the impulse given to the particles by the irregularities during the mirroring is along the line of force, the resulting particle convection velocity is the component of the solar wind velocity along the field direction, or

$$j_{convection} = N V_o \left(1 + \frac{\Omega^2 r^2}{V_o^2}\right)^{-1/2} \hat{b} \tag{13b}$$

where b is a unit vector along the local field direction. Finally there is a macroscopic current due to the particle drift normal to the field direction. Since we are here interested in the mean drift velocity of all particles, rather than guiding centers, in a unit volume, we must use the current density

$$\vec{j}_{drift} = N\vec{V}_{drift} = N \frac{\vec{B}}{B^2} \times \left(- \vec{E} + \frac{\nabla p}{eN}\right) = N \frac{\vec{B}}{B^2} \times \left(- \vec{E} + \frac{2\mathcal{E}}{3Ne} \nabla N\right) \tag{13c}$$

rather than equation 1, (see Spitzer (1962)). As before, $E = - V_o \times B$.

The Fokker-Planck equation then becomes

$$\frac{\partial N}{\partial t} + \nabla \cdot \left[- K \nabla_b N + N V_o \left(1 + \frac{\Omega^2 r^2}{V_o^2}\right)^{-1/2} \hat{b} + N \vec{V}_{drift} \right] + \frac{\partial}{\partial \mathcal{E}} (N \dot{\mathcal{E}}) = 0 \tag{14}$$

where $\bar{V}_{drift}$ and $\dot{\mathcal{E}}$ are given in equations 9a and 13c. It seems worth pointing out that equation 13b and 13c imply that in the absence of diffusion, particles stream radially outward from the sun at large r, but that this is due to electric field drift and not convection.

Rather than attempting to solve equation 14, we shall adopt an approximate treatment of the combined diffusion and drift which essentially amounts to first solving the diffusion problem without drift and then calculating the drift of the particles as though they were propagating outward at their diffusion velocities. Near the sun ($\Omega r \ll V_o$) we have that $j_{conv} \approx N V_o \hat{b}$, $|V_{drift}| \ll V_o$ and $\dot{\mathcal{E}}$ is small. Furthermore, approximating that the diffusion is along the r direction and ignoring the divergence of space with increasing r, equation 14 lead simply to

$$\frac{\partial N}{\partial t} + V_o \frac{\partial N}{\partial r} - K \frac{\partial^2}{\partial r^2} N = 0 \tag{14a}$$

Following Parker (1965) the solution of equation 14a corresponding to the boundary conditions that

$$N(o,t,\mathcal{E}) = 0 \quad \text{and} \quad N(r,0,\mathcal{E}) = n(\mathcal{E})\,\delta(r-\lambda)$$

is

$$N(r,t,\mathcal{E}) = \frac{n(\mathcal{E})}{(4\pi Kt)^{1/2}} \left[1 - \exp\left(-\frac{r\lambda}{Kt}\right)\right] \exp\left[-\frac{(V_o t + r)^2}{4Kt}\right] \tag{15}$$

By differentiation with respect to time it follows that (for $r\lambda \ll Kt$) t_m, the time at which most particles with K arrive at r, is

$$t_m = - \frac{3K + (9K^2 + V_o^2 r^2)^{1/2}}{V_o^2} \tag{15a}$$

and therefore a diffusion velocity may be defined as

$$V_D^m = \frac{dr}{dt_m} = (9\frac{K^2}{r^2} + V_o^2)^{1/2} \tag{15b}$$

for these particles. Particles arriving at r in the time t have diffused more rapidly by the factor, $\frac{t_m}{t}$, and may therefore be characterized by an average diffusion velocity,

$$V_D = (\frac{t_m}{t})\, V_D^m \tag{16}$$

We have therefore replaced the statistical diffusion of the particles by a steady outward propagation at the diffusion velocity in this approximation. It is now possible to estimate the drift of the diffusing particles, and according to equation 12, the azimuthal drift becomes

$$\phi' = - \frac{t}{t_m} \int_{r_o}^{R_e} \frac{\Omega^3 r^2 \, dr}{V_o^2 \, (1 + \frac{\Omega^2 r^2}{V_o^2}) \, (9\frac{K^2}{r^2} + V_o^2)^{1/2}} \equiv (\frac{\Delta\phi'_m}{t_m})\, t \tag{17}$$

Consequently the above change of independent variable from t to ϕ' in equation 15 gives the azimuthal intensity distribution, $N(R_e, \phi', \mathcal{E})$, to

IV. Quantitative Results

We shall now use the relationships obtained above to calculate the amount of particle drift, deceleration and the form of the azimuthal particle intensity distribution. The drift of particles in the polar direction is given by equation 9, where the drift velocity may be written as

$$\dot{R}_\theta = \frac{2 \times 10^8 \Omega \mathcal{E}}{V_o B_e R_e^2 \left(1 + \frac{\Omega^2 R_e^2}{V_o^2}\right)^{-1/2}} \cdot \frac{r^2}{\left(1 + \frac{\Omega^2 r^2}{V_o^2}\right)^2} ; \tag{18}$$

$\mathcal{E}$ is in ev, B_e is in gauss, R_e is in cm, and Ω is in sec $^{-1}$. Expanding the diffusion velocity, equation 15b, in the power series

$$V_D = \begin{cases} \frac{3K}{r}\left[1 + \frac{1}{2}\left(\frac{V_o r}{3K}\right)^2\right] & \text{for } 3K > V_o R_e \\ V_o & \text{for } 3K \ll V_o R_e \end{cases} \tag{19}$$

equation 9 becomes

$$\frac{d\theta'}{dr} = \begin{cases} \frac{12 \times 10^8 (\mathcal{E}_o - c\theta') K}{V_o B_e R_e^2 \left(1 + \frac{\Omega^2 R_e^2}{V_o^2}\right)^{-1/2}} \cdot \frac{r^2}{\left(\frac{V_o^2}{\Omega^2} + r^2\right)^2 \left(\frac{18K^2}{V_o^2} + r^2\right)} & \text{for } 3K > V_o R_e \\ \\ \frac{2 \times 10^8 (\mathcal{E}_o - c\theta')}{V_o^2 B_e R_e^2 \left(1 + \frac{\Omega^2 R_e^2}{V_o^2}\right)^{-1/2}} \cdot \frac{r}{\left(1 + \frac{\Omega^2 r^2}{V_o^2}\right)^2} & \text{for } 3K \ll V_o R_e \end{cases} \tag{20}$$

where equation 8 has been used. Ignoring the dependence of K on θ', equation 20 integrates to

$$\mathcal{E}_f = \mathcal{E}_o - c\theta' \tag{21}$$

$$= \begin{cases} \mathcal{E}_o \exp\left[\dfrac{-24\times 10^{16}\, V_o K \left\{ \left(\dfrac{V_o^2}{\Omega^2} - \dfrac{18K^2}{V_o^2}\right) \dfrac{r}{2\left(\dfrac{V_o^2}{\Omega^2} + R_e^2\right)} + \dfrac{\left(\dfrac{V_o^2}{\Omega^2} + \dfrac{18K^2}{V_o^2}\right)}{2V_o/\Omega} \tan^{-1} \dfrac{\Omega R_e}{V_o} - \dfrac{\sqrt{18}K}{V_o} \tan^{-1} \dfrac{V_o R_e}{\sqrt{18}K} \right\}}{B_e R_e^2 \Omega^3 \left(1 + \dfrac{\Omega^2 R_e^2}{V_o^2}\right)^{-1/2} \left(\dfrac{V_o^2}{\Omega^2} - \dfrac{18K^2}{V_o^2}\right)^2} \right] \\ .39\, \mathcal{E}_o, \quad \text{for } 3K \ll V_o R_e \end{cases}$$

The diffusion coefficient may be expressed as

$$K = \begin{cases} 10^{10}\lambda & \text{for relativistic electrons} \\ .43 \times 10^{8} \lambda\, \mathcal{E}_o^{1/2} & \text{for non-relativistic protons} \end{cases}$$

and choosing $\lambda = 2 \times 10^{11}$ cm, $V_o = 300$ km/sec, the final energy $\mathcal{E}_f(\mathcal{E}_o)$ and the drift, $\theta'(\mathcal{E}_o)$ may be evaluated. These functions are shown in Figure 2. The flat relative energy loss for the electrons and low energy protons is a reflection of the fact that these particles have transit times which are energy independent, and the protons, having longer transit times, lose a larger fraction of their energy. The actual amount of drift is seen to be small for all particles in the energy range of interest. Therefore although this drift could in principle produce a "charge separation" of protons and electrons, the angular separation is very small under the prevailing conditions.

We next evaluate the azimuthal drift of the particles. According to equations 12 and 19, the location of the particles relative to the field structure is found from

$$\Delta\phi'_m = -\frac{1}{V_o^2}\int_{r_o}^{R_e}\frac{\Omega^3 r^2 dr}{\left(1+\frac{\Omega^2 r^2}{V_o^2}\right)\frac{V_o^2}{6Kr}\left(\frac{18K^2}{V_o^2}+r^2\right)}, \quad \text{for } 3K > V_o R_e \tag{22}$$

Integrating, one obtains (23)

$$\phi'_m = \frac{3K\Omega}{V_o^2\left(\frac{V_o^2}{\Omega^2}-\frac{18K^2}{V_o^2}\right)}\left[\frac{V_o^2}{\Omega^2}\ln\left(1+\frac{\Omega^2 R_e^2}{V_o^2}\right)-\frac{18K^2}{V_o^2}\ln\left(1+\frac{V_o^2 R_e^2}{18K^2}\right)\right]$$

which has the value

ϕ'_m = .34 radians for protons

= .02 radians for electrons

at $\mathcal{E}_o$ = 1 Mev. That is, if 1 Mev protons and electrons are ejected from the sun onto a given line of force, one should expect that the protons will have drifted some 20^o to the east of the line of force by the time they reach 1 AU whereas the electron will stay essentially tied to the line of force.

The form of the azimuthal particle intensity distribution follows from equations 15 and 17. Letting $N(\phi',K)$ represent the intensity of particles with diffusion coefficient K arriving at the azimuth ϕ', we have

$$\mathcal{N}(\phi',K) = N(t,K)\,\frac{dt}{d\phi'} = \left(\frac{t_m(K)}{\phi'_m(K)}\right)\,N(t,\phi')\,) \tag{24}$$

which is evaluated for 1 Mev and 30 Mev protons in Figure 3, with $n(\mathcal{E}) = \mathcal{E}^{-4}$. The peak of the distribution for 1 Mev protons is understandably at a larger angle than for the 30 Mev protons since they drift azimuthally during a longer transit time. (It should be recalled at this point that, contrary to the polar drift velocity, the azimuthal drift velocity, equation 11, does not depend upon particle energy. The increased drift for the 1 Mev protons is thus a reflection of the longer transit time only.)

V. Azimuthal Variation of Energy Spectrum

We now restrict ourselves to protons and examine the effects of propagation on the energy spectrum. The variation of the energy spectrum with azimuth can be studied by obtaining the time variation of the spectral slope at some fixed energy. Referring to equations 15a and 23, we find that $\frac{t_m(K)}{\phi'_m(K)}$ is very nearly energy independent. Thus, confining ourselves to times and energies for which $Kt \gg R_e\lambda$, equation 24 becomes

$$\mathcal{N}\,(\phi',t,\mathcal{E}) \propto \mathcal{E}^{-4.75}\; t^{-1.5} \exp\left[\frac{-(V_o t + R_e)^2}{3.48 \times 10^{17}\,\mathcal{E}^{1/2}}\right] \frac{t}{\phi'}$$

where $K = .87 \times 10^{17}\,\mathcal{E}^{1/2}$ and $t = (\frac{t_m}{\phi_m'})\,\phi'$. Transforming to logarithms we obtain

$$m = \frac{d(\log \mathcal{N})}{d(\log \mathcal{E})} = -4.75 + \frac{9 \times 10^{14}\,(t + 5 \times 10^5)^2}{6.96 \times 10^{17}\,\mathcal{E}^{1/2}\,t} \tag{25}$$

This time variation is displayed in Figure 4 at three energies. (In Figure 4 and elsewhere we use three variables which must be distinguished: t is a transit time for particles passing between the sun and $R_e = 1$ AU, ϕ' is an azimuthal angle measured from the magnetic sector boundary along which the particles are injected, and $\mathcal{T} = \frac{27}{2\pi}\,\phi'$ is the time elapsed since the sector boundary swept past the earth.) In Figure 5, curve a, the energy spectrum at $\mathcal{T} = 3$ days is plotted as an example of a propagation-modulated spectrum. The following conclusions may be drawn from these curves.

(1) Only <u>differences</u> in slope at different energies or times are of significance since the spectral index of the injection spectrum appears additively in equation 25. (2) The spectrum has the characteristic behavior of falling rapidly to a maximum steepness after approximately 2 days and then flattening very gradually with increasing time. This time dependence reflects the fact that high energy particles, having the shortest transit times, are found closest to the sector boundary ($\tau \sim 0$) while lower energy particles predominate more and more at greater distances from the sector boundary. At the solar wind transit time of 5.7 days ($\tau \sim 2$ days) the maximum intensity of low energy particles arrives (with the solar wind) and the energy spectrum is therefore steepest. For larger values of τ, the plasma carrying the low energy particles is beyond 1 AU and one is observing particles which have diffused inward, in the rest frame of the plasma. Therefore as τ increases one detects particles which have retrogressed progressively farther and farther from the plasma and these are the higher energy particles. The energy spectrum therefore flattens again. (3) The time variation described above becomes less pronounced at higher energies because $\frac{dV_o}{d\mathcal{E}}$ ($= \frac{d^2 r}{dt_m d\mathcal{E}}$), how rapidly the transit time varies with energy, decreases with increasing energy. Therefore at high energies, where all particles have nearer the same transit times, the particles tend to maintain their initial energy spectrum as they propagate outward.

In this discussion, as in equation 24, the variation of the spectrum due to deceleration has been ignored. Without solving for the energy spectrum resulting from the coupled diffusion and energy loss in the present calculation, we simply indicate the effect of deceleration alone on the spectrum. If we suppose that the energy spectrum at the sun is $n(\mathcal{E}) = \mathcal{E}_o^{-4}$

and all particles arrive simultaneously at 1 AU with energies $\mathcal{E}_f = g(\mathcal{E}_o)$, given by equation 21 then their energy spectrum becomes

$$n'(\mathcal{E}_f) = n(\mathcal{E}_o)\frac{1}{\frac{dg}{d\mathcal{E}_o}}$$

This spectrum is plotted in Figure 5, curve b, and it may be seen that the deceleration is sufficiently small so that the spectrum is modulated very little. We conclude therefore that the energy spectrum observed at the earth should rather resemble the energy spectrum at injection except at early times ($\tau \sim 0$) and very low energies ($\mathcal{E}_f \lesssim 1$ Mev).

VI. Application to Imp I Data

We now turn to the data obtained from the Imp I satellite collected in Figure 1. The integral intensity profile for Mev protons is shown at the bottom and these recurrent shapes are to be compared with the predicted profile, Figure 3. The general features of a steeper ascent than descent and a peak intensity about two days after the boundary seem to be reflected in the data. Furthermore, Fan et al, (1966) report that the energy spectrum is slightly flatter (E^{-4}) during the first days of the sector than in the last days (E^{-5}), and this is consistent with the predicted slope variation, Figure 4. Therefore it seems that if the sun released protons only along the sector boundary observed on 4 December and was inactive elsewhere, then the subsequent diffusion and drift of these particles would give rise to intensity profiles and energy spectra similar to those observed.

The observed intensity profile for Mev electrons indicates that maxima occur three days or more beyond the 12 December sector boundary. However, our analysis predicts that solar electrons released from the sun along that sector boundary should be observed predominantly at the boundary, and therefore we conclude that the observed electrons have not had such an origin.

Let us now consider the alternative idea (Brunstein, 1965) that the electrons are galactic. In Figure 1 the variation of the solar wind velocity across the field sectors is displayed. Let us assume that this variation persists for a distance ΔR beyond the earth. Then if the inward diffusion of cosmic rays is largely confined to the spiral field direction so that the cosmic ray density along a given line of force depends only upon the local wind velocity, the modulation, given by Parker (1965), is

$$n_E = n_o \exp\left[-\frac{3V\,\Delta R}{\beta c\,\lambda}\left(1 + \frac{1}{3}\left(\frac{\Omega\Delta R}{V}\right)^2\right)\right] \tag{26}$$

where n_E is the flux at the earth, n_o is the flux beyond ΔR and V is the variable wind speed. Choosing the values $\lambda = 2 \times 10^{11}$ cm, $\Delta R = 1$ AU, $\beta c = c$ and $\Omega\Delta R = 400$ km/sec, one finds that the percent change in the galactic intensity corresponding to a wind velocity change dV should be

$$\frac{dn_E}{n_E} \simeq - 3 \times 10^{-4}\, dV \tag{27}$$

However the observed percentage changes indicated in Figure 1 ($\sim$30%) are much larger than one would expect from equation 27, which predicts that a solar wind variation of 100 km/sec should produce only a 3% change in the electron intensity. In order to quantitatively examine the extent to which the daily variations obey equation 26, we have studied the daily correlation between the electron intensity and the plasma velocity. In Figure 6 the correlation coefficient for various detectors is plotted as a function of delay time between the particle intensity and plasma velocity records, and it may be seen that the electron intensity shows no significant correlation with the plasma velocity for any value of the delay. This suggests that the modulation described by equation 26 cannot alone describe the propagation of the observed electrons.

If equation 26 is applied to 50 Mev protons, having $\beta \simeq .3$, one obtains

$$\frac{dn_E}{n_E} \simeq - 10^{-8}\,dV \qquad (28)$$

assuming the same parameter values as for equation 27. Thus a solar wind variation of 100 km/sec is predicted to produce a 10% variation in the cosmic ray intensity, and the data does indeed indicate such variations. The daily correlation between the cosmic ray intensity and the plasma velocity is indicated in Figure 6 for each of four Imp I detectors (described by Balasubrahmanyan et al, 1965) and the Deep River neutron monitor. In each case the data reveals a statistically significant correlation which is strongest when the cosmic ray data is compared with the plasma data of the previous day. However there is weaker, yet statistically significant, correlation for time delays ranging from $\sim$ +1 to -5 days between the cosmic ray and plasma velocity records. Without attempting to provide a detailed interpretation of these time delays in this paper, we only comment that negative delays are to be expected since the electric field drift (section III) causes the particles to lag slightly behind the field lines about which they are guiding. Such a field line, characterized by a certain plasma velocity, therefore crosses the earth before the cosmic rays associated with that field line, in agreement with the negative delay in Figure 6. The only point we wish to make at this time, however, is that the cosmic rays follow the transient behavior of the plasma velocity while the electrons do not. Since neither the model based on solar origin described earlier, nor the modulation model, equation 26, explain these electrons, it would seem that perhaps processes are operating on electrons which have little effect on the heavier cosmic rays.

Summary

The interplanetary electromagnetic field, in a reference frame at rest with respect to the earth, has been represented by an Archimedes spiral magnetic field and the electric field induced by the solar wind. It is found that charged particles ejected from the sun drift in these fields in such a way that they tend to co-rotate with the magnetic field while being decelerated by the electric field. At the same time the particles diffuse along the magnetic field lines and arrive at 1 AU with a dispersion in transit times which in turn implies a dispersion in the drift. Making the simplifying approximation that the diffusion is one dimensional with a constant mean free path equal to $\sim$.01 AU, proton intensity profiles and energy spectra have been calculated, and it is found that these predictions are in reasonable agreement with the recurrent proton data from the Imp I satellite. Also, the cosmic ray data from Imp I was found to correlate well with the daily variations in the solar wind velocity. This implies that a "stream" of low energy cosmic rays is essentially always in the presence of one and the same plasma velocity and hence, one and the same bundle of field lines.

Acknowledgments

We wish to thank Drs. D. Guss and A. Lenchek of the University of Maryland as well as Drs. U. Desai, F. B. McDonald and R. Palmiera of the Goddard Space Flight Center for helpful discussions. One of us (G.S.) wishes to thank Dr. A. Lenchek in particular for his critical reading of the manuscript. This work was supported in part by NASA grant NsG-695.

References

1. Axford, W. I., Anisotropic Diffusion of Solar Cosmic Rays, Planet. Space Sci., 13, 1301-1309, 1965.

2. Balasubrahmanyan, V. K., G. H. Ludwig, F. B. McDonald and R. A. R. Palmeira, Results from the Imp I GM Counter Telescope Experiments, J. Geophys. Res., 70, 2005-2019.

3. Bridge, H., A. Egidi, A. Lazarus, E. Lyon and L. Jacobson, Peliminary Results of Plasma Measurements on Imp A., Space Research V, North Holland (1965).

4. Brunstein, K. A., Possible Source Mechanism for Low Energy Galactic Electron, Phys. Rev. 137, 3B, 8 February, 1965.

5. Cline, T. L., G. H. Ludwig and F. B. McDonald, Detection of Interplanetary 3 to 12 Mev Electrons, Phys. Rev. Letters, Dec. 28, 1964.

6. Fan, C.Y., Gloeckler, G. and Simpson, J. A., Protons and Helium Nuclei Within Interplanetary Magnetic Regions Which Corotate with the Sun, Proceedings of the International Congress on Cosmic Rays, London, 1966.

7. Northrop, T. G., The Adiabatic Motion of Charged Particles, Interscience, New York, 1963.

8. Parker, E. N., Interplanetary Dynamical Processes, Interscience, New York, 1963.

9. Parker, E. N., The Passage of Energetic Charged Particles Through Interplanetary Space, Planet. Space Sci., Vol. 13, 9-49, 1965.

10. Roelof, E. C., Diffusion of Solar Protons and Electrons in the Interplanetary Magnetic Field (to be published).

11. Spitzer, L., Physics of Fully Ionized Gases, Interscience, New York, 1962.

12. Wilcox, J. M. and Ness, N. F., Quasistationary Corotating Structure in the Interplanetary Medium, J. Geophys. Res., 70, 5793-5805.

Figure Captions

Figure 1. Imp I data, November, 1963-January, 1964. The vertical lines indicate magnetic sector boundaries and the crosshatching represents the interval of uncertainty in these boundaries. The first sector was characterized by an outward directed field and the succeeding sectors alternate in polarity.

Figure 2. Energy loss and polar drift of solar charged particles. This energy loss is caused by the gradient drift of particles against the induced electric field of the solar wind.

Figure 3. Predicted intensity-time profiles for solar protons. The intensity is plotted against time measured from sector boundary passage. The corresponding angular position is also indicated.

Figure 4. Predicted time variation of the spectral index for solar protons. The spectral index at each energy is plotted against time (and angular position) as in Figure 3.

Figure 5. Representative differential energy spectrum for solar protons. Curve a represents the energy spectrum at $\tau = 3$ days resulting from propagation without energy loss for an injection spectrum E_o^{-4}. Curve b represents the energy spectrum resulting from energy loss only, for the injection spectrum, E_o^{-4}.

Figure 6. The time correlation between observed particle intensity and solar wind velocity. The linear correlation coefficient is plotted against delay time between particle intensity and plasma velocity records. Positive delay indicates that the particle intensity was correlated with the plasma velocity measured at an earlier time. $T_{\perp}$, $T_{\parallel}$, C (plastic scintillator) and omnidirectional intensity and electrons (3-12 Mev) represent measurements made with the Imp I satellite.

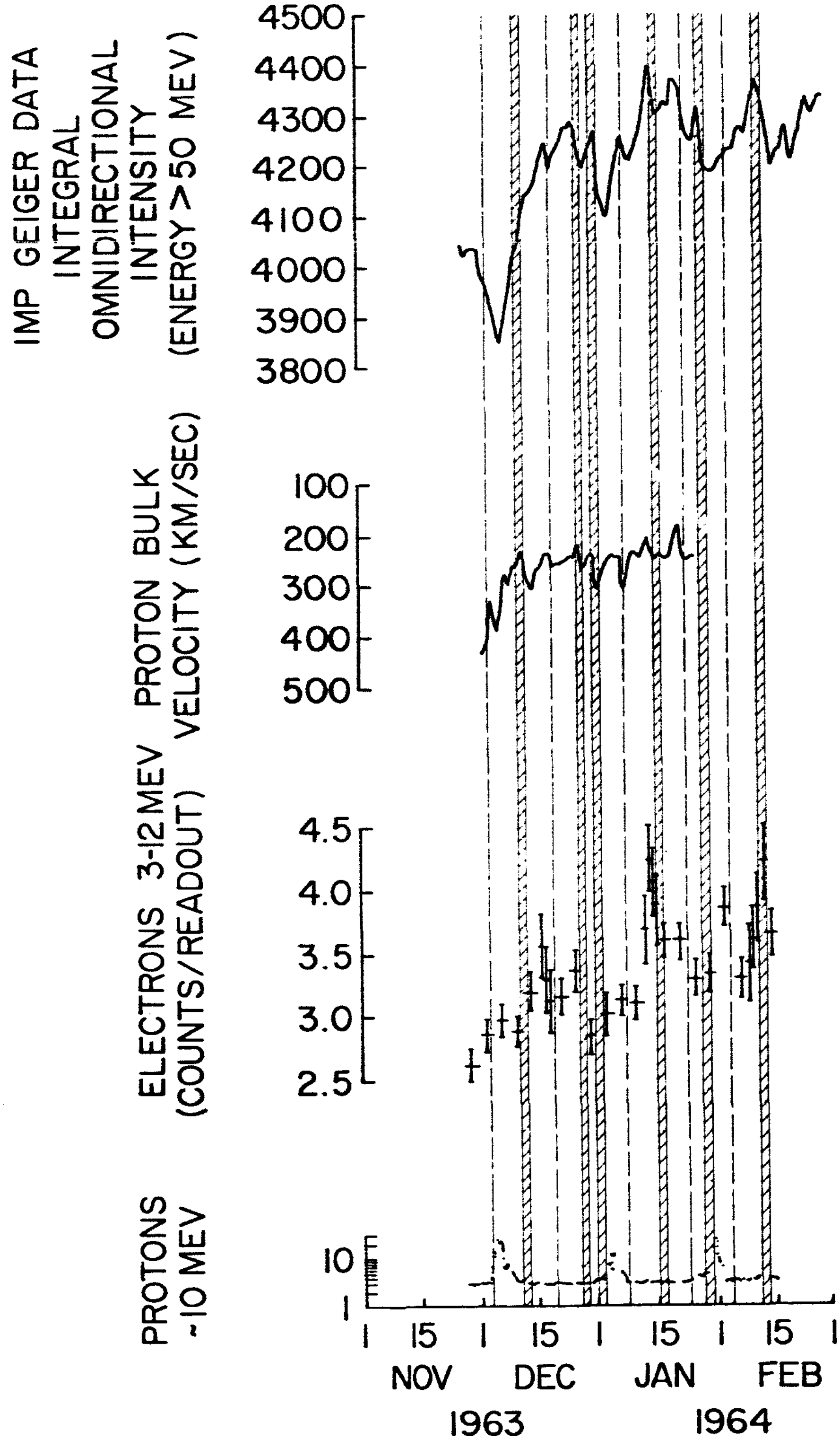

IMP GEIGER DATA
INTEGRAL
OMNIDIRECTIONAL
INTENSITY
(ENERGY > 50 MEV)
4500
4400
4300
4200
4100
4000
3900
3800
PROTON BULK
VELOCITY (KM/SEC)
100
200
300
400
500
ELECTRONS 3-12 MEV
(COUNTS/READOUT)
4.5
4.0
3.5
3.0
2.5
PROTONS
~10 MEV
10
1
1
15
1
15
1
15
1
15
1
NOV
DEC
JAN
FEB
1963
1964

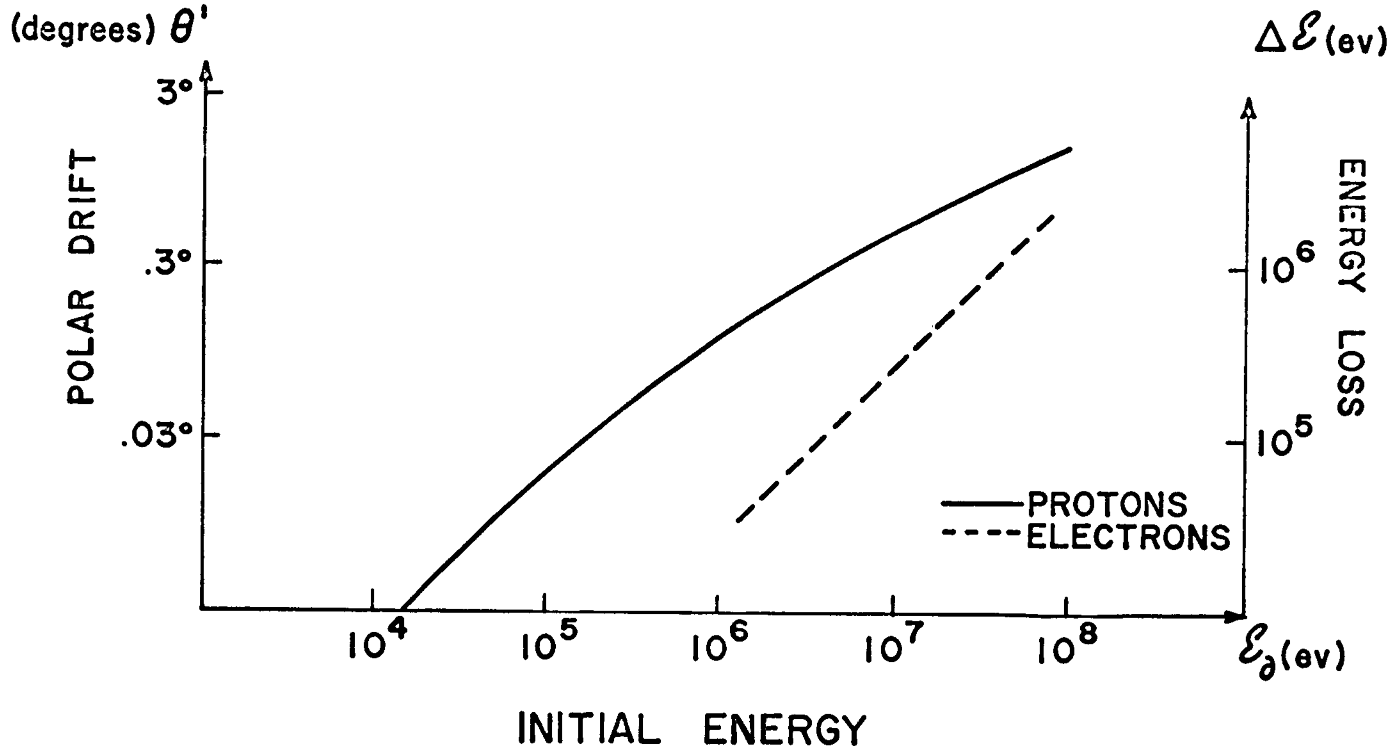

(degrees) θ'
3°
.3°
.03°
POLAR DRIFT
Δℰ (ev)
ENERGY LOSS
10^6
10^5
PROTONS
ELECTRONS
10^4
10^5
10^6
10^7
10^8
ℰ∂ (ev)
INITIAL ENERGY

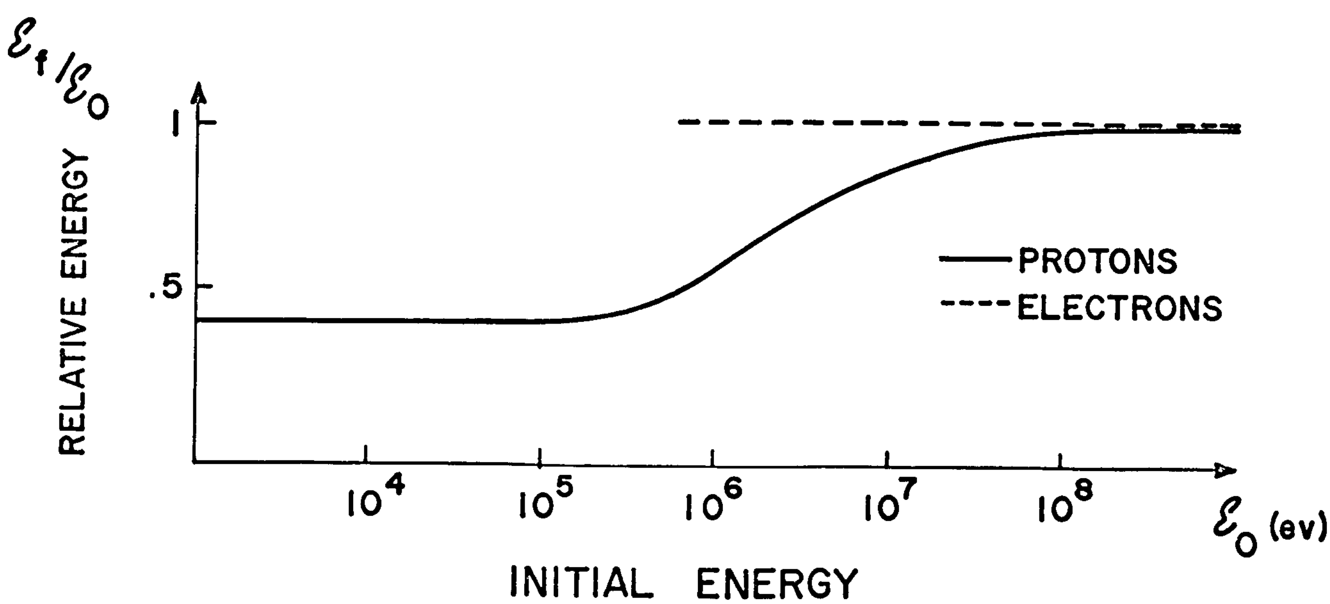

ℰf / ℰ0
1
.5
RELATIVE ENERGY
PROTONS
ELECTRONS
10^4
10^5
10^6
10^7
10^8
ℰ0 (ev)
INITIAL ENERGY

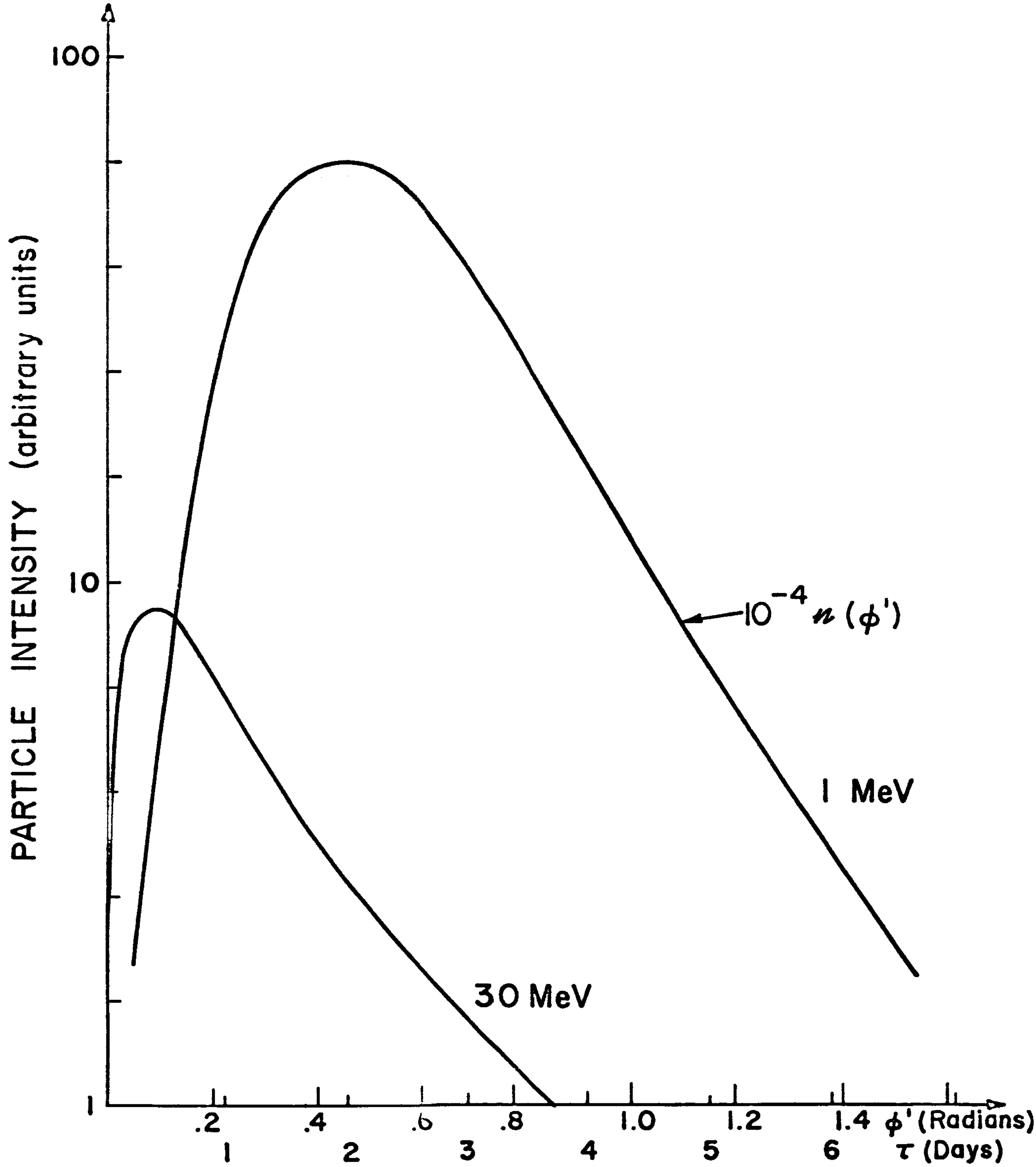

PARTICLE INTENSITY (arbitrary units)
100
10
1
$10^{-4}\,n\,(\phi')$
1 MeV
30 MeV
.2
.4
.6
.8
1.0
1.2
1.4
ϕ' (Radians)
1
2
3
4
5
6
τ (Days)

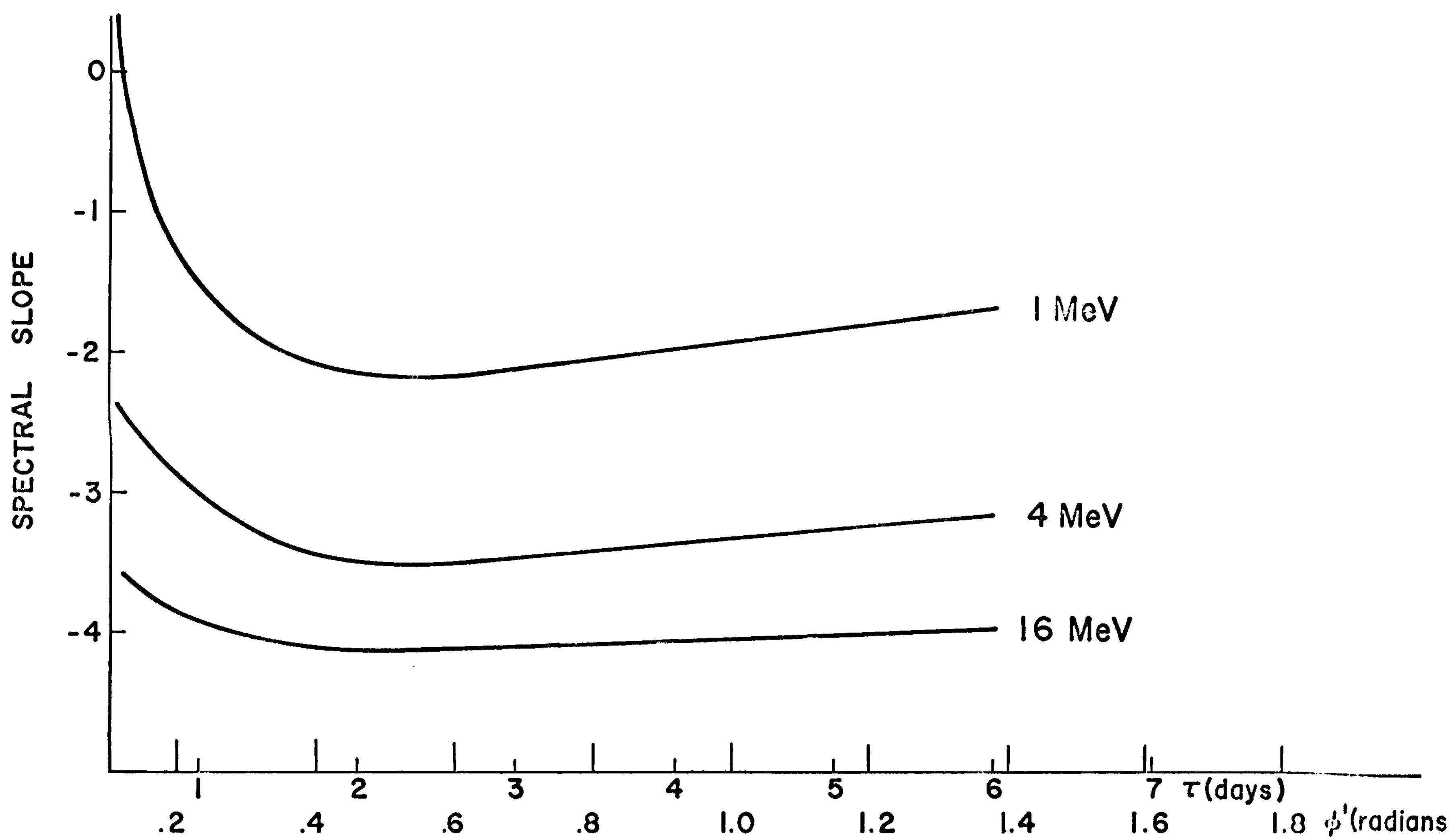

SPECTRAL SLOPE
0
-1
-2
-3
-4
1 MeV
4 MeV
16 MeV
1
2
3
4
5
6
7 τ(days)
.2
.4
.6
.8
1.0
1.2
1.4
1.6
1.8 φ'(radians

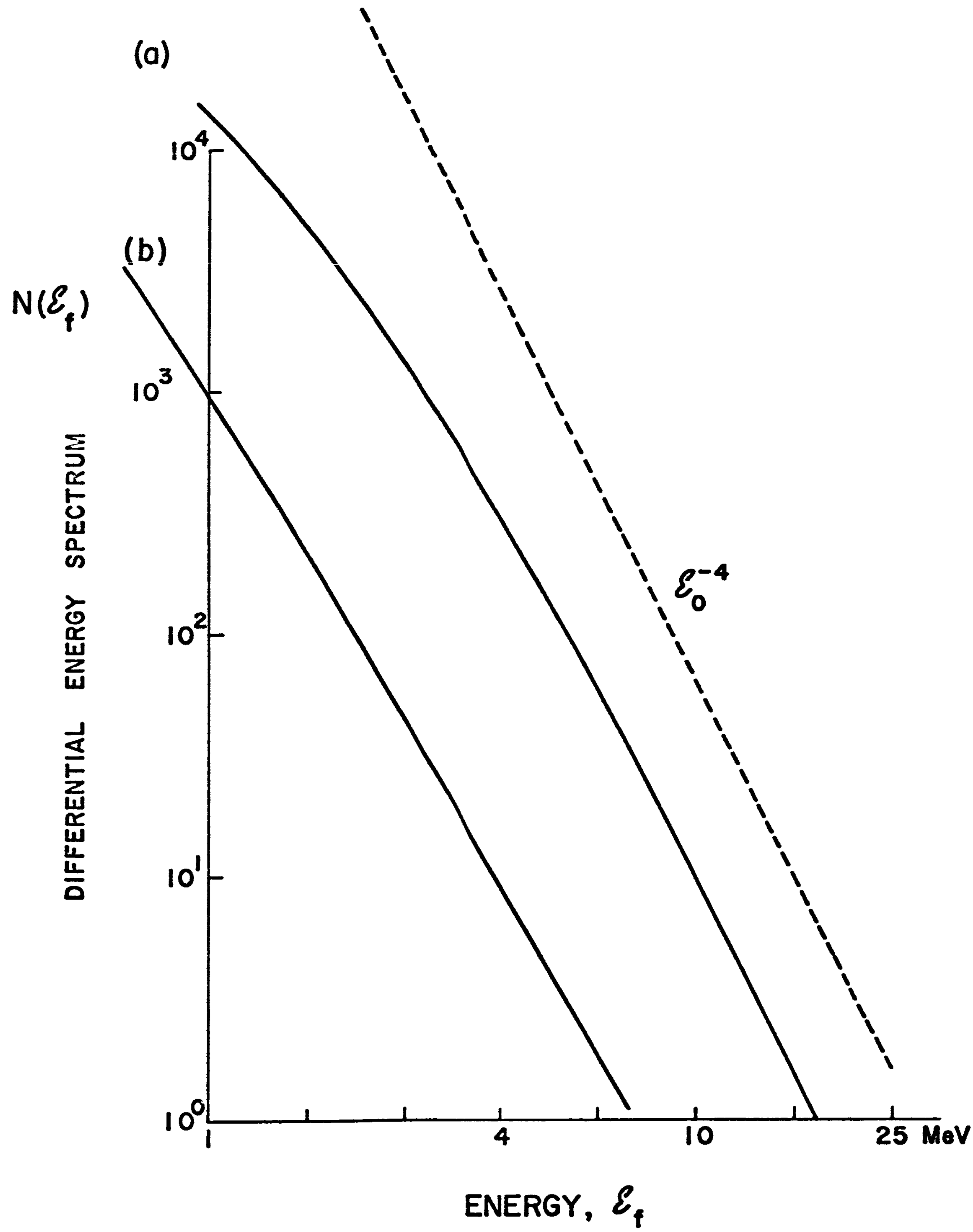
(a)
(b)
N($\mathcal{E}_f$)
DIFFERENTIAL ENERGY SPECTRUM
10^4
10^3
10^2
10^1
10^0
$\mathcal{E}_0^{-4}$
1
4
10
25 MeV
ENERGY, $\mathcal{E}_f$

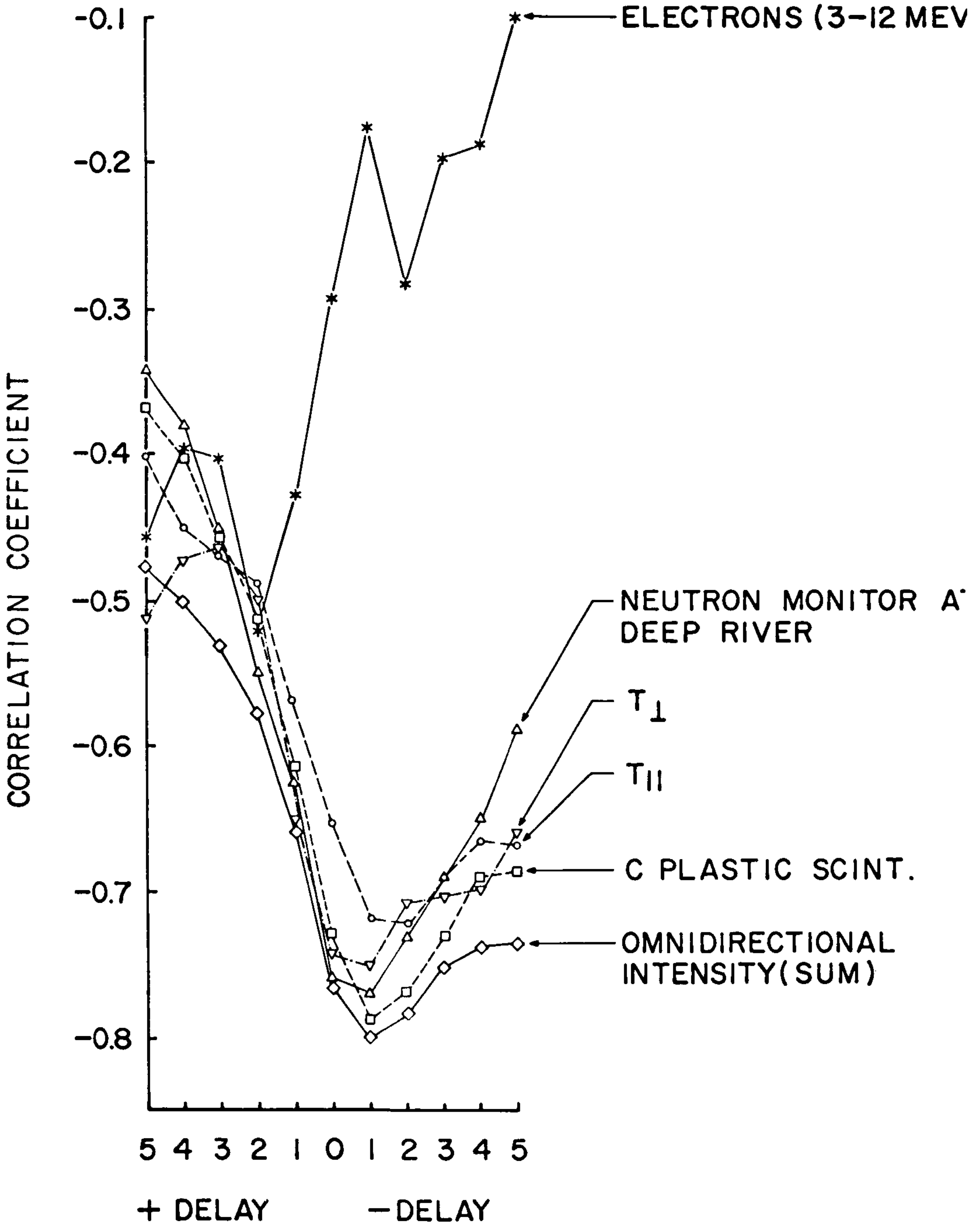

CORRELATION COEFFICIENT
-0.1
-0.2
-0.3
-0.4
-0.5
-0.6
-0.7
-0.8
ELECTRONS (3-12 MEV
NEUTRON MONITOR A
DEEP RIVER
$T_{\perp}$
$T_{\parallel}$
C PLASTIC SCINT.
OMNIDIRECTIONAL
INTENSITY (SUM)
5 4 3 2 1 0 1 2 3 4 5
+ DELAY
− DELAY